

Computer Aided Diagnosis of Breast Nodule Detection Using Deep Learning Technique

K.M. Abubakkar Sithik and Dr.S. Kother Mohideen

***Abstract---** Now a days, a breast cancer is one of the leading causes of cancer-related death in the industrialized countries and it has the least favorable prognosis among various cancer types. Breast cancer is the fourth most common cause of cancer related deaths in the Western countries. Tumor specimens contain a variety of healthy cells as well as cancerous cells, and this heterogeneity underlies resistance to various cancer therapies. In this study we aim to facilitate early detection of the breast cancer by finding minimal set of genetic biomarkers that can be used for establishing diagnosis. In this paper, we propose a Neural networks approach using paired histopathology and immunofluorescence images (for label),and demonstrates classification prediction power. This method can solve current issue on discrepancy between genomic- or transcriptomic-based and pathology-based tumor purity estimates by improving histological evaluation.*

***Keywords---** Histogram Equalization, Feature Extraction, Segmentation, Neural Networks.*

I. INTRODUCTION

A patient complaining of sudden onset of epigastric pain radiating to the back, associated with nausea and vomiting, requires rapid exclusion of a wide range of life-threatening conditions involving the cardiovascular (myocardial infarction, ruptured, and/or dissecting aortic aneurysm) and gastrointestinal (peptic ulcer disease with perforation or bleeding) systems. The clinician's history and examination findings are augmented by relevant investigations in narrowing the differential diagnoses to eventually guide the management and treatment of a certain condition and its associated complications. Mammogram is an X-ray picture of the breast. Mammography is the type of mammogram that are used to check the breast cancer which have no symptoms. It can also help to reduce the number of deaths from breast cancer among women from ages 40 – 70. There are many commonly used images segmentation algorithms. This paper mainly describes the following five algorithms for simple analysis. The first is the threshold segmentation method. Threshold segmentation is one of the most commonly used segmentation techniques in region-based segmentation algorithms. Its essence is to automatically determine the optimal threshold according to a certain criterion, and use these pixels according to the gray level to achieve clustering. Followed by the regional growth segmentation. The basic idea of the regional growth algorithm is to combine the pixels with similar properties to form the region, that is, for each region to be divided first to find a seed pixel as a growth point, and then merge the surrounding neighborhood with similar properties of the pixel in its area. Then is the edge detection segmentation method. Edge detection segmentation algorithm refers to the use of different regions of the pixel gray or color discontinuity detection area of the edge in order to achieve image segmentation. The next is the segmentation based on clustering. The algorithm based on clustering is based on the similarity between things as the criterion of class division, that is, it is divided into several subclasses according to the internal structure of the

*K.M. Abubakkar Sithik, Research Scholar, Bharathiyar University, Coimbatore, Tamil Nadu. E-mail: abubakkar.sithik@rediffmail.com
Dr.S. Kother Mohideen, Associate Professor & Research Head, PG Research Department of IT, Sri Ram Nallamani Yadava College of Arts and Science, Tenkasi, Tamil Nadu. E-mail: drskmkother@gmail.com*

sample set, so that the same kind of samples are as similar as possible, and the different are not as similar as possible. The last is the segmentation based on weakly-supervised learning in CNN. It refers to the problem of assigning a semantic label to every pixel in the image and consists of three parts. 1) Give an image which contains which objects. 2) Give the border of an object. 3) The object area in the image is marked with a partial pixel. At present, from the international image segmentation method, the specific operation of the process of segmentation method is very diverse and complex, and there is no recognized a unified standard. This paper discusses and compares the above four methods, and learns from the shortcomings to analyze better solutions and make future forecasts.

II. LITERATURE SURVEY

Russoet al (1998) proposes the two algorithms for classification of tissue histology based on representations of morphometric context. These methods are modelled the context of the morphometric information based on pixel- or patch-level features. The morphometric features at various locations and scales are based on spatial pyramid matching framework. Due to the effectiveness the morphometric features achieve excellent performance even with small number of training samples across different segmentation strategies and independent datasets of tumors. This method is highly extensible to different tumor types, robust in the presence of large amounts of technical and biological variations and invariant to different cell arrays.

Altoet al (2003) proposes a new method for a single nucleus classification using deep learning. A spatially constrained convolutional neural network that are used to detect and classify nuclei. In order to provide a large amount of labeled data, immune fluorescence (IF) images used as label information instead of pathologists' annotations. Then, a large dataset and train a convolutional neural network are constructed to classify cancerous and normal cells at a single-cell level. Chenget al (2003) proposes a novel method to establish the breast cancer classifier. Firstly, the concept of quantum and fruit fly optimal algorithm (FOA) are introduced. Then FOA is improved by quantum coding and quantum operation, and a new smell concentration determination function is defined. Finally, the improved FOA is used to optimize the parameters of support vector machine (SVM) and the classifier is established by optimized SVM. Chenget al (2006) suggests to obtain the minimum set of biomarkers that can be used for detection of breast cancer. The Genetic algorithm (GA) has applied on PDAC data to classify tissue samples. This algorithm provides a list of biomarkers that play the most important role in this lethal disease as a by-product. Petersenet al (2012) establishes a spectral clustering algorithm. Breast ductal adenocarcinoma is one of most aggressive malignancy. The high dimensional PDAC gene expression dataset in Gene Expression Omnibus (GEO) database, is analyzed in this work. In this work, after pre-processing of the data, we have used three types of spectral clustering methods, Normalized, Ng-Jordan and proposed entropy-based Shi-Malik spectral clustering algorithms to find important genetic and biological information. There we have applied new Shannon's Entropy based distance measure to identify the clusters on breast dataset. Some Biomarkers are identified through KEGG Pathway analysis. The Biological analysis and functional correlation of genes based on Gene Ontology (GO) terms show that the proposed method is helpful for the selection of Biomarkers.

Contrast enhanced ultrasound (CEUS) and contrast enhanced computer tomography (CECT) diagnosis and

histology in patients presenting to a tertiary referral center are detected breast masses by standard abdominal ultrasound. Contrast enhanced ultrasound (CEUS) demonstrated a good performance for detection and characterization of solid breast lesions using both a transabdominal and an endoscopic approach by Krizhevsky et.al (2012). Moschopoulos et.al (2013) proposed a novel method for automatic threshold for segmenting MRI images, if images with poor contrast there may be a chance of losing information in boundaries to overcome that problem. Here, homogeneity criterion and probability are calculated for each pixel for getting the more accuracy segmentation for gray matter or white matter MRI datasets.

Paceet al. (2014) proposed a method for implementing a texture feature-based computerized method for segmenting limb using SRG algorithm for segmenting the breast parenchyma from breast CT images based on the region of interest (ROI). A new texture feature-based seeded region growing algorithm is proposed for automated segmentation of organs in abdominal MR images. The proposed texture feature-based automated SRG algorithm on abdominal organ segmentation. The benefit of this algorithm is obvious, as it provides a parameter-free production environment to allow minimum user intervention. This can be especially helpful for batch work or to novice computer users. Wanget al. (2016) proposed a new method and application tool for liver volume and evaluation of the left over function of the liver former to the involvement of the surgeons devoted for patient with persistent kidney disease liver volume segmentation, visualization, and virtual cutting for liver CT scan images is done. For CT image segmentation multi seeded region growing technique is used. Lee et al. (2017) planned MRI breast tumor segmentation for that they developed a customized automatic seeded region growing based on Particle Swarm Optimization (PSO) image clustering system has been presented. For pre-processing level set active contour and morphological thinning methodologies are used. Here, PSO clusters intensities are involved in the automated SRG initial seed and threshold value selection. The SRG algorithm for tumour segmentation is chosen because it is fast, simple and robust. The chosen image clustering method is PSO-based, because it produces better results compared with other clustering methods such as K-means, Fuzzy C-means, K-Harmonic means and Genetic Algorithms. Laghmatiet al. (2019) presented an automatic segmentation of brain lesions from diffusion-weighted magnetic resonance imaging using region growing approach. Similarity measure pixel intensity and pixel mean values differences are used to detect the lesion region using region splitting and merging and for automation process the thresholding technique is used. Yanget al. (2019) implemented an automatic seeded region growing algorithm for effectual pixel labeling technique and an automatic seed selection method for segmentation process. A seed tracking algorithm is also proposed for automatic moving object extraction. It is used for detecting the uncovered background and new objects which also located inside the temporal change mask like the moving objects.

III. PROPOSED METHOD

Generally, a CAD system consists of several steps as follows (1) image enhancement, (2) image segmentation, (3) feature extraction, (4) feature classification, and finally, (5) an evaluation for the classifier. The novelty of this work is to extract the ROI using two techniques and replace the last fully connected layer of the DCNN architecture with SVM.

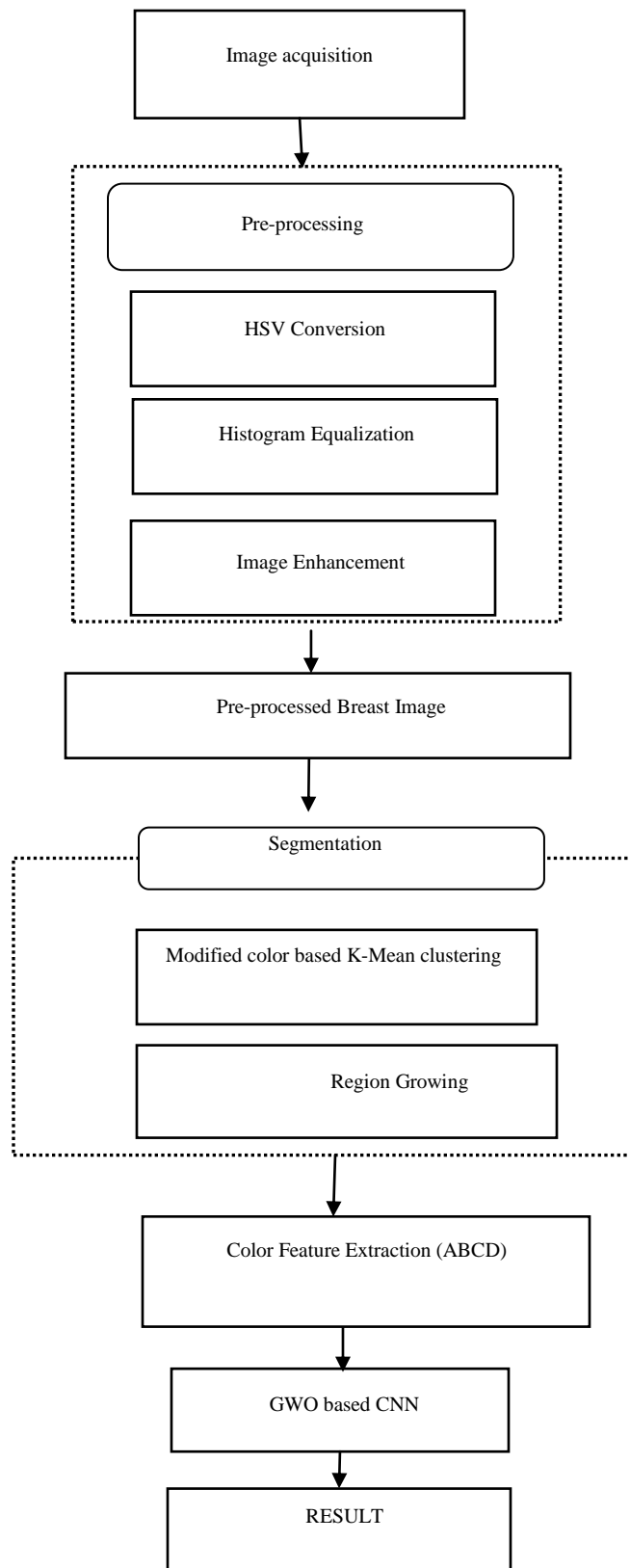


Figure 3.1: Block Diagram for Breast Tumor

For example, the image can be equalized to emphasize certain features or remove other features. With filtering, the image processing is implemented which includes Sharpening, Smoothing and edge enhancement. In the acquired image, poor contrast is one of the defects. The Improved Linear Iterative Clustering method technique is used for enhance the breast image.

After the segmentation of breast image, the tumor affected part in the breast can be clearly found out by applying several post processing operations. Only the part of the image can be viewed by applying some basic operations that is the part of the image having more intensity and more area. From the image collection, the local features were extracted and then by using the Adjustable surface normal overlap segmentation algorithm, they were clustered typically for content based image retrieval in the classification. The visual words which is called as the computer cluster centers and then form a codebook, which forms an indexing newly added images as a basis. The local features were extracted from the best fitting visual words and the local features were extracted and assigned. In the existing image collection, the new image is added. The local features in distribution, which indicates the local feature histogram over the former computed cluster, which serves as the new image for the computed cluster. Similar images were retrieved by using the CNN.

3.1 Preprocessing

Pre-processing is the process of removing noise from the original image. Various type of noise is present because of the disturbance. Initially the input images is read after that convert the color space model (HSV) the noise is removed with the help of modified color based histogram equalization method. Finally image enhancement output is obtained.

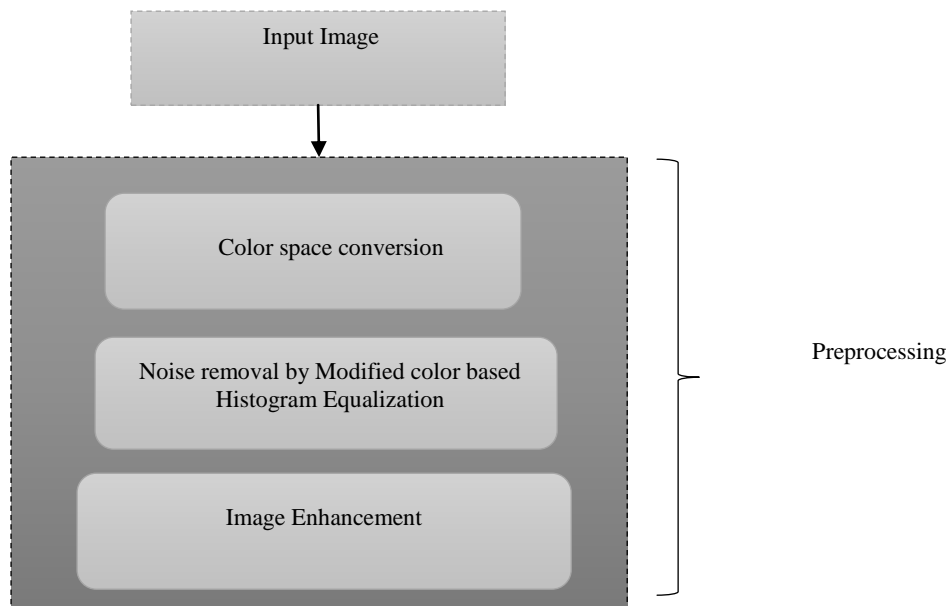


Figure 3.2 Block Diagram of Preprocessing System

3.1.1 Image Acquisition

The term breast tumor or tumor is mostly characterized as an intracranial neoplasm. They are produced as a result of an uncontrolled and abnormal cell division. This type of cell division is found to occur in blood vessels, breast envelopes, lymphatic tissues and in the cranial nerves. Even as result of cancer, the breast tumor can be produced. Rise in Blood Pressure in breast and changing of breast tissue can be harmed because of tumor. These were the manifestations which impacts the reason for the breast tumor.

3.1.2 Pre-Processing

In order to improve the quality of the images, the MRI images can be preprocessed. The tumors are then detected with the help of morphological operation. The image is thereafter analyzed and is proceeded with the noise reduction technique and image enhancement technique. Few assumptions reflecting the appearance of the cancer are subjected to the morphological operation and as a result the tumor is formulated to the color scale image with some intensity and then finally the image is made evident in tumor.

Steps involved in preprocessing:

- Conversion to color space model
- High pass filter
- Filter mask
- Image enhancement

3.1.3 High Pass Filter

Once image is converted to color image, it is inputted to HPF. For basis of most sharpening methods high pass type of filter is used. When contrast is enhanced between adjoining areas, with little variation in brightness or darkness, the image is sharpened. In the high pass filter the frequency is decreased which helps to keep the image with high frequency information. HPF is used to improve the center pixel kernel's brightness. A single positive value is found in the center of the kernel array that is totally enclosed by negative values.

3.1.4 Filter Mask

The technique called filter mask, which is used to enhance the image or modify the image. For example, the image can be filtered to emphasize certain features or remove other features. With filtering, the image processing is implemented which includes Sharpening, Smoothing and edge enhancement.

3.1.5 Image Enhancement

In the acquired image, poor contrast is one of the defects.

- The MRI image of breast is read as an input.
- By changing the image mode, the color components were removed to color image.
- The images in the edges were made to be clear and the components were sharpened by crisp.
- By applying the median filter, the quality of image is enhanced.
- By plotting the histogram, the intensity of the distribution of the pixel were analyzed and studied.

3.2 Histogram Equalization

Histogram equalization is a method in image processing of contrast adjustment using the image's histogram. Histogram equalization often produces unrealistic effects in photographs; however it is very useful for scientific images like thermal, satellite or x-ray images, often the same class of images to which one would apply false-color. Also histogram equalization can produce undesirable effects when applied to images with low color depth.

There are two ways to think about and implement histogram equalization, either as image change or as palette change. The operation can be expressed as $P(M(I))$ where I is the original image, M is histogram equalization mapping operation and P is a palette. If we define a new palette as $P'=P(M)$ and leave image I unchanged then histogram equalization is implemented as palette change. On the other hand, if palette P remains unchanged and image is modified to $I'=M(I)$ then the implementation is by image change. In most cases palette change is better as it preserves the original data.

Algorithm

1. Create the histogram for the image.
2. Convert the input image into a grayscale image.
3. Find frequency of occurrence for each pixel value i.e. histogram of an image.
4. Calculate Cumulative frequency of all pixel values.

$$cdf(x) = \sum_{j=1}^x h(j)$$

5. Divide the cumulative frequencies by total number of pixels and multiply them by maximum graycount (pixel value) in the image.
6. Calculate the new values through the general histogram equalization formula.

$$eh(i) = round\left(\frac{cdf(i) - cdf_{min}}{M \times N - cdf_{min}} * (L - 1)\right)$$

7. Assign new values for gray value in the image.
8. Get the histogram and cumulative histogram of the new image.
9. `OutputIm = histoeq(InputImage,nbins,minvalue,maxvalue,display)`

3.3 Segmentation

In computer vision, image segmentation is the process of partitioning a digital image into multiple segments. Image segmentation is typically used to locate objects and boundaries (lines, curves, etc.) in images. More precisely, image segmentation is the process of assigning a label to every pixel in an image such that pixels with the same label share certain characteristics. In this technique, canny edge detection and region based detection are involved.

Steps Involved in Proposed Algorithm

The different advances engaged with the proposed segmentation algorithm is as demonstrated as follows

1. Set the Input image
2. Get k values
3. Distance between pixels and cluster centers are calculated
4. Each pixel is allotted to the adjacent cluster center
5. The mean value is computed i.e. for each cluster calculate the cluster
6. Check in case of any distinction in cluster centers
7. If so, proceed from the step 3 by captivating new mean as cluster centers
8. If not so, at that point process the measurements and detachable data output cluster sectioned image.

3.3.1 Canny Edge Detector

Canny edge detector is an edge detection operator that uses a multi-stage algorithm to detect a wide range of edges in images. Canny edge detection is a technique to extract useful structural information from different vision objects and dramatically reduce the amount of data to be processed. It has been widely applied in various computer vision systems. Canny has found that the requirements for the application of edge detection on diverse vision systems are relatively similar. Thus, an edge detection solution to address these requirements can be implemented in a wide range of situations. The general criteria for edge detection include:

1. Detection of edge with low error rate, which means that the detection should accurately catch as many edges shown in the image as possible.
2. The edge point detected from the operator should accurately localize on the center of the edge.
3. A given edge in the image should only be marked once, and where possible, image noise should not create false edges.

To satisfy these requirements Canny used the calculus of variations – a technique which finds the function which optimizes a given functional. The optimal function in Canny's detector is described by the sum of four exponential terms, but it can be approximated by the first derivative of a Gaussian.

Among the edge detection methods developed so far, Canny edge detection algorithm is one of the most strictly defined methods that provides good and reliable detection. Owing to its optimality to meet with the three criteria for edge detection and the simplicity of process for implementation, it became one of the most popular algorithms for edge detection.

Process of Canny Edge Detection Algorithm

The Process of Canny edge detection algorithm can be broken down to 5 different steps:

1. Apply Gaussian filter to smooth the image in order to remove the noise.
2. Find the intensity gradients of the image.

3. Apply non-maximum suppression to get rid of spurious response to edge detection.
4. Apply double threshold to determine potential edges.
5. Track edge by hysteresis: Finalize the detection of edges by suppressing all the other edges that are weak and not connected to strong edges.

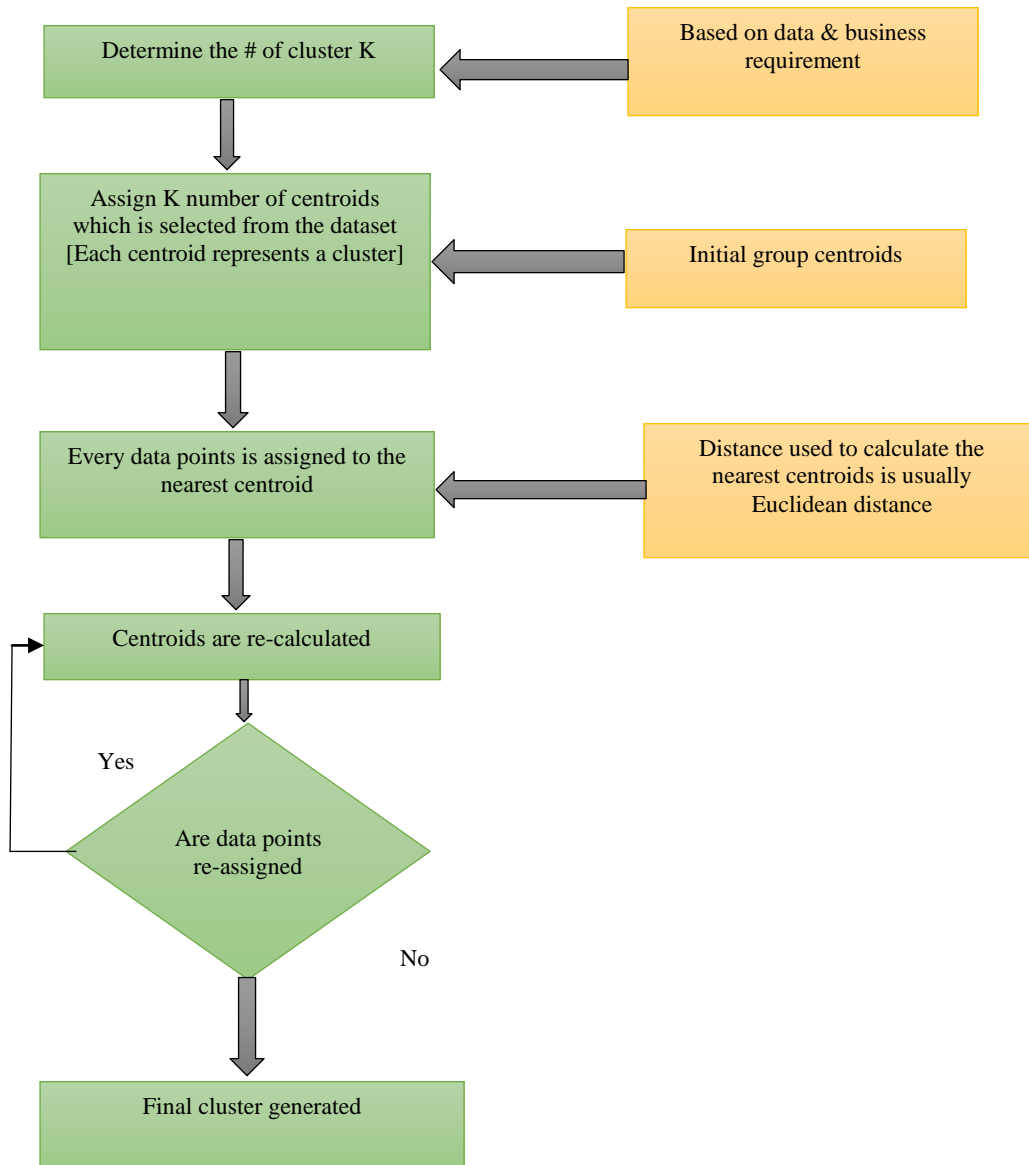


Figure 3.3: Flowchart of Region based Segmentation

3.3.2 Region based Segmentation

Region growing is a simple region-based image segmentation method. It is also classified as a pixel-based image segmentation method since it involves the selection of initial seed points. This approach to segmentation examines neighboring pixels of initial seed points and determines whether the pixel neighbors should be added to the region.

The process is iterated on, in the same manner as general data clustering algorithms. The region-based segmentation is simpler than other methods. It divides the image into different regions based on predefined criteria. There are two main types for the region-based segmentation; (1) region growing and (2) region splitting and merging.

The region-growing algorithm has the ability to remove a region from an image based on some predefined criteria such as the intensity. Region growing is an approach to image segmentation in which neighboring pixels are examined and joined to a region class where no edges are detected. It is also classified as a pixel-based image segmentation method as it involves the selection of initial seed point. It should be noted that the region splitting and merging method is the opposite of the region growing method as it works on the complete image. In this manuscript, the region of interest (ROI) is extracted from the original mammogram image by two different methods. The first step to extract the ROI is to determine the tumor region by a threshold value, which is a value determined with respect to the red color pixel. After some trials, the threshold was set to 76 for all the images regardless of the size of the tumor. Then, the biggest area within this threshold along the image was determined and the tumor was cropped automatically.

If the region growing process is finished, then the region merging process begins. Different regions of an image are merged to form a single region with some similarity criterion. Region growing algorithm is a simple technique which can efficiently separate the pixels in an image having similar properties. Region growing segmentation scheme can be described using the properties as shown in equation 3.2

$$\bigcup_{i=1}^n R_i = R \quad (3.2)$$

Where R_i is the i^{th} region in an image R , and the image is divided into n regions as shown in equation 3.3.

$$R_i \cap R_j = \emptyset \quad (3.3)$$

The regions R_i and R_j are disjoint.

$$p(R_i \cup R_j) = False \quad (3.4)$$

For any logical predicate P defined over two adjacent regions are false. Similarity, it is required that the region R_i is a connected region.

This method receives a predefined set of seed pixels along with the input image and these seed pixels point to the objects to be segmented. The seed pixel is compared to all unallocated neighboring pixels in the image and this enables the region to grow iteratively. δ is the measure of similarity, which is defined as the difference between mean of pixels is measured.

Advantages

1. Region growing methods can correctly separate the regions that have the same properties we define.
2. Region growing methods can provide the original images which have clear edges with good segmentation results.
3. Disadvantages
4. Computationally expensive.
5. It is a local method with no global view of the problem.

6. Sensitive to noise.
7. Unless the image has had a threshold function applied to it, a continuous path of points related to colour may exist which connects any two points in the image.

Algorithm: Region Growing Algorithm

1. Initialize the number of seed points, $R_1, R_2, R_3, \dots, R_n$.
2. Initialize Seed points, p_1, P, p_3, \dots, P_n .
3. Compute the difference δ between initial seed pixel p_i and neighbouring pixel. If delta is less than threshold T , the neighbouring pixel will be assigned to region I .
4. Re-compute ne boundary for each regions and the pixels in the boundary are the new seed pixels
5. Repeat step 2 to 5, until all the pixels are allocated to suitable regions.

3.3.3 Initialization of Seed Pixels

The segmented regions of Seeded Region Growing (SRG) have high texture similarity and do not contain fragments. However, the drawbacks are initialization of seed-points and computational time required for convergence. The problem with initialization of seed-points is that, if different sets of initial seed points must be very similar to its neighboring pixels. At least one seed pixel should be generated for every expected region in the image. There should not be any connection between seeds of individually regions.

In this work, seed selection is performed based on the occurring frequency and merging. Initially the color levels in the image are computed and arranged in ascending order. Then the frequency of occurrence of each color level is calculated. Then the first pixel is assigned as the first seed point finally the pixels are merged to obtain optimum seed points.

3.3.4 Initialization of Threshold

First, we search the maximum intensity I_{min} from the image. Secondly, we calculate the mean intensities of the background and foreground on the basis of threshold T_{old} .

$$T_{old} = \frac{I_{max} + I_{min}}{2} \tag{3.5}$$

$$I_{bm} = \frac{\sum_{I(x,y) < T_{old}} I(x,y)}{\sum_{I(x,y) < T_{old}} N(x,y)} \tag{3.6}$$

$$I_{fm} = \frac{\sum_{I(x,y) \geq T_{old}} I(x,y)}{\sum_{I(x,y) \geq T_{old}} N(x,y)} \tag{3.7}$$

The new threshold is given by,

$$T_{new} = \frac{I_{bm} + I_{fm}}{2} \tag{3.8}$$

Where, I_{bm} is the intensity of the background, I_{fm} is the mean intensity of the foreground, $I(x,y)$ is intensity of pixel and $N(x,y)$ is the number of pixels.

3.4 Feature Extraction

Feature extraction a kind of dimensionality decrease that productively speaks to fascinating parts of an image as

a conservative component vector. This methodology is valuable when image sizes are expansive and a lessened component portrayal is required to rapidly total assignments, for example, image coordinating and recovery. In image recovery system, include extraction is critical advance to depict the image with least number of descriptors. All images comprise of visual examples, surface properties, and scene. From this image shading, surface and shape, features of an image were separated for likeness coordinating. Deep learning feature extraction is involved in this proposed method. There are several variations on CNNs layers architecture: Convolutional Layer, Pooling Layer and Fully-Connected Layer. Fully-Connected Layer is just acting as neural network. CNN algorithm has two main processes: convolution and sampling, which will happen on convolutional layers and max pooling layers.

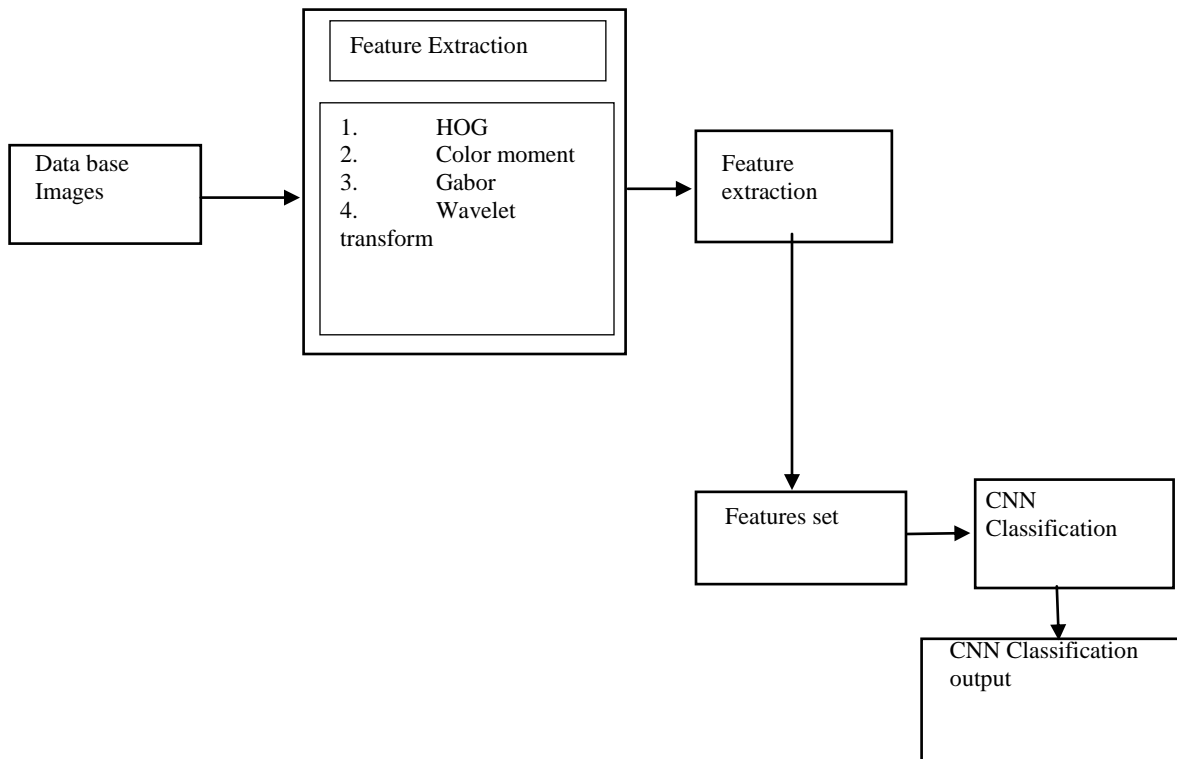


Figure 3.4: Block Diagram of Feature Extraction

After performing similarity matching done to obtain the result that is similar. On the other hand proceed the same step from query images and compare both the feature extraction result of the query and image database. Finally obtain the retrieved image.

A. Image Acquisition: For reading input image in lung data set, the input images should be pre-processed using HSV color space

B. Extracting Features: feature extraction method is the best part in CBRSIR system. The extracted features are separated and to obtain the better result. Here, four features are extracted. The proposed feature is HOG, and the remaining features are color moment, Gabor and wavelet transform.

i). HOG Features

The proposed feature extraction method is HOG feature. This feature are very simple, and used for various applications. In the first step, the point of image is detected using Harris detector. After calculating the points, the pixel is set by 16 X 16. Initially the region is splitted into 4 X 4 regions. The HOG features can be defined below,

$$h(k) = \sum d_{x,y} \in e_k m_{x,y} \tag{1}$$

$$m_{x,y} = \sqrt{dx^2 + dy^2} \tag{2}$$

$$d_{x,y} = \arctan \frac{dy_{x,y}}{dx_{x,y}} - D \tag{3}$$

$$dx_{x,y} = I_{x,y} - I_{x,y+1} \tag{4}$$

$$dy_{x,y} = I_{x,y} - I_{x,y+1} \tag{5}$$

$$D = \arctan \frac{\sum d_{x,y} dy_{x,y}}{\sum dx_{x,y}} \tag{6}$$

Where, $I_{x,y}$ is the x, y pixel value of each sub-region, $m_{x,y}$ is the gradient magnitude, $d_{x,y}$ is the gradient direction

ii). Color Moment Feature

In CBIR system, color moment feature extraction is a low level color feature, HOG provides only the texture information of the image. While encoding, we can improve the power of color index using inclusion algorithm. Initially the original image is divided into non-overlapping of three regions. In this way to extract the features from non-overlapping sub-regions. The color moment features are extracted by using the below equations.

$$E_i = \frac{1}{N} \sum_{y=1}^N S_{x,y} \tag{7}$$

$$\sigma_i = \left[\frac{1}{N} \sum_{y=1}^N (S_{x,y} - E_x)^2 \right]^{\frac{1}{2}} \tag{8}$$

Where, The value of the x^{th} color moment at the y^{th} image pixel is $S_{x,y}$.

iii). Gabor Feature

The simplest extraction method used in image processing is Gabor features. This Gabor feature extraction algorithm can be classified into two types which contain spatial time domain and spatial frequency domain.

iv). Wavelet Transform Feature (WT)

Wavelet Transform (WT) is a resolution-oriented feature in multiscale function. It analyzing different resolution level of images.

3.5 Classification

A neural network is a system of interconnected artificial “neurons” that exchange messages between each other. The connections have numeric weights that are tuned during the training process, so that a properly trained network will respond correctly when presented with an image or pattern to recognize. The network consists of multiple layers of feature-detecting “neurons”. Each layer has many neurons that respond to different combinations of inputs from the previous layers. Convolution Neural Network (CNN) is a deep learning technique. CNNs are used in variety of

areas, including image and pattern recognition, speech recognition, natural language processing, and video analysis. There are a number of reasons that convolutional neural networks are becoming important. In traditional models for pattern recognition, feature extractors are hand designed. In CNNs, the weights of the convolutional layer being used for feature extraction as well as the fully connected layer being used for classification are determined during the training process. The improved network structures of CNNs lead to savings in memory requirements and computation complexity requirements and, at the same time, give better performance for applications where the input has local correlation (e.g., image and speech).

3.4.1 GWO based CNN

GWO algorithm was simulation about social hierarchy and group hunting behavior of grey wolf population, through tracking, encircling, hunting, attacking of wolf population and other processes to achieve the optimization of intelligent algorithm. The Improved GWO algorithm has the advantages of simple principle, few parameters to be adjusted, easily to implement and strong capability to global search.

The GWO algorithm is used to optimize the continuous function, the number of grey wolves is set to N , and the solution search space is set to d dimension. The location of the i wolf is defined in the d dimension space, and α is the current best individual in the grey wolf population, β and δ are individual grey wolves whose fitness value rank in second and third, respectively. The global optimal solution of the optimization problem is the location of the final prey.

In the GWO algorithm, it is necessary to determine the distance between the individual and the prey is shown in the equation (3.9)

$$D = |C \cdot X_p(t) - X(t)| \quad (3.9)$$

Where $X(t_p)$ represents the location of the prey at the time of t -th generation;

$X(t)$ represents the location of the grey wolf individual at the time of t -th generation; Constant C is the swing factor is shown in the equation (3.10)

$$C = 2r_1 \quad (3.10)$$

Where, r_1 is a random number from 0 to 1. The position updating formula of grey wolf is shown in the equation (3.11)

$$X(t+1) = X(t) - A \cdot D \quad (3.11)$$

Where, A is the convergence factor is shown in the equation (3.12)

$$A = 2a_2 - a \quad (3.12)$$

Where r_2 is a random number from 0 to 1, while, a linearly decreases from 2 to 0 as the number of iterations increases.

In order to simulate the hunting behavior of the grey wolf, suppose α wolf, β wolf and δ wolf have a better understanding to the location of the prey, so the grey wolf population can use the position of the three to decide the location of the prey. When the wolves get the prey location information, leader wolf α command β and δ to hunt.

The grey wolf population to update its position according to the location information of α , β and δ wolf are is shown in the equation

$$D_\alpha = |C_1 \cdot X_\alpha(t) - X(t)| \quad (3.13)$$

$$D_\beta = |C_2 \cdot X_\beta(t) - X(t)| \quad (3.14)$$

$$D_\delta = |C_3 \cdot X_\delta(t) - X(t)| \quad (3.15)$$

$$X_1 = X_\alpha - A_1 \cdot D_\alpha \quad (3.16)$$

$$X_2 = X_\beta - A_2 \cdot D_\beta \quad (3.17)$$

$$X_3 = X_\delta - A_3 \cdot D_\delta \quad (3.18)$$

$$X_p(t+1) = \frac{X_1 + X_2 + X_3}{3} \quad (3.19)$$

Where, according to the formula (3.13)–(3.19), the distance between the individual in the population and the wolf, β wolf and δ wolf is calculated, and the distance and direction of the individual moving to the prey are determined by the formula.

The optimization process of GWO a algorithm is that a group of gray wolves in the search space randomly generated, in the process of evolution, the position of the prey is evaluated and located by α , β and δ wolf, and the rest of individual in the group to calculate the distance between themselves and their prey, they complete the Omni-directional proximity, encirclement, attack, and so on, and finally capture the prey.

GWO-CNN is based on classification works on hunting strategy of grey wolves and their leadership quality. Based on the leadership and hunting strategy, GWO are divided into four categories such as alpha (α), beta (β), omega (δ).

- The training procedure of Algorithm 1 is described below:

Step 1: D is taken as input.

Step 2: For each image I_1^{tr} in D^{tr} of D compute the color features and they can be determined as F_{l,c_i}^{tr} for extracting the texture features, F_{l,T_j}^{tr} can be determined and for the shape features, F_{l,S_k}^{tr} can be determined, where $i = 1, 2, \dots, n_c, j = 1, 2, \dots, n_T, k = 1, 2, \dots, n_s$:

Step 3: For each image I_1^{tr} in D^{tr} of D each of n_d distance formulas is calculated for finding the distances of color features, texture features, and shape features for two different images I_1^{tr} and I_v^{tr} the distances calculation is given below:

$$d_{l,c_i}^{tr} = (F_{l,c_i}^{tr}, F_{v,c_i}^{tr}), d_{l,T_j}^{tr} = (F_{l,T_j}^{tr}, F_{v,T_j}^{tr}), \text{ and } d_{l,S_k}^{tr} = (F_{l,S_k}^{tr}, F_{v,S_k}^{tr}),$$

Where I_v^{tr} indicates the v^{th} image of the training set D^{tr} in D, $l \neq v, l, v \in \{1; 2, \dots, m_{tr}\}$

Step 4: For D^{tr} in D, // GWO proceed for each epoch

For each solution k // for each parameter set, (Φ_k, w_k)

For each $I_1^{tr} \in D^{tr}$ // for all training images

call Image Retrieval ($D, n_g, \Phi_k, w_k, I_1^{tr}$)

Loop

compute the fitness for (Φ_k, w_k) which is the average of precision rates for each I_1^{tr} .

save parameters G best and P best which have the highest fitness during each epoch.

Loop

save G best in (Φ_0, w_0) .

Loop

Step 5: Output (Φ_0, w_0) , where

$$\Phi_0 = F_{c_{i_0}}^{tr}, d_{c_0}^{tr}, (F_{T_{j_0}}^{tr}, d_{T_0}^{tr}), (F_{S_{k_0}}^{tr}, d_{S_0}^{tr})\}$$

$$w_0 = (w^C, w^T, w^S)$$

• For retrieving the images from the input image, 'Image Retrieval Algorithm' is used .by setting the parameters and determines the extraction in the training phase for the query image and the Output of most similar images in an ascending can be determine.

Step 1: If $n_g = 1$ then $D^g = D^\Omega \parallel D^\Omega = D$

Step 2: Set the parameters with Φ_k, W_k

Step 3: For a query image $I_q \in D^{te}$, three determined extraction methods in the training phase are utilized to compute three kinds of features $F_{q,c_{i_0}}^{te}, F_{q,T_{j_0}}^{te}$ and $F_{q,S_{k_0}}^{te}$.

$$F_q^{te} = (F_{q,c_{i_0}}^{te}, F_{q,T_{j_0}}^{te}, F_{q,S_{k_0}}^{te})$$

Step 4: For each $D^{g,te}$ in D^g of D

$$d_{l,c_0}^g = (F_{l,c_{i_0}}^g, F_{q,c_{i_0}}^g), d_{l,T_0}^g = (F_{l,T_{j_0}}^g, F_{q,T_{j_0}}^g), \text{ and } d_{l,S_0}^g = (F_{l,S_{k_0}}^g, F_{q,S_{k_0}}^g)$$

Step 5: For each D^g in D

For each $I_l^g \in D^g$

Compute the similarities $\Delta_{l,q}^g$ between I_l^g and I_q using the following similarity function $\Delta(I_l^g, I_q)$,

$$\Delta_{l,q}^g = \Delta(I_l^g, I_q) = (w^C, w^T, w^S)(d_{l,c_0}^g, d_{l,T_0}^g, d_{l,S_0}^g)$$

Where t denotes the transpose operation for the vectors.

Step 6: Sort the similarities $\Delta_{l,q}^g$ by an ascending order.

Step 7: Output several most similar images in an ascending fashion.

$$\Delta_{l,q}^g = \Delta(I_l^g, I_q) = (w^C, w^T, w^S)(d_{l,c_0}^g, d_{l,T_0}^g, d_{l,S_0}^g)$$

The training phase of Algorithm 2 is determined, by taking the input for each subset.

Step 1: Input D.

Step 2: For each subset D^g in D

For each image $I_l^{g,tr} \in D^{g,TR}$ of D^g

Compute three kinds of features, $F_{l,C_i}^{g,tr}$, $F_{l,T_j}^{g,tr}$, and $F_{l,S_k}^{g,tr}$

where $i = 1, 2, \dots, n_c$, $j = 1, 2, \dots, n_t$; $k=1, 2, \dots, n_s$.

Step 3: For each subset D^g in D

For each image $I_l^{g,tr} \in D^{g,TR}$ of D^g each of n_d distance formulas is employed to

Compute distances of three kinds of features for two different images $I_l^{g,tr}$ and $I_v^{g,tr}$, where $I_v^{g,tr}$ indicates the v th image of the training set of the g th category

in $D^{g,TR}$ of D, $l \neq v, l, v \in \{1; 2, \dots, m_{g,TR}\}$. Three distances can be computed by the following formulas.

$$d_{l,C_i}^{g,tr} = (F_{l,C_i}^{g,tr}, F_{v,C_i}^{g,tr}), d_{l,T_j}^{g,tr} = (F_{l,T_j}^{g,tr}, F_{v,T_j}^{g,tr}), \text{ and } d_{l,S_k}^{g,tr} = (F_{l,S_k}^{g,tr}, F_{v,S_k}^{g,tr})$$

Step 4: For each $D^{g,TR}$ in D^g of D // GWO procedure

set (1/3,1/3,1/3) to (w^c, w^T, w^s) .

For each epoch

For each solution k

For each $I_l^{g,tr} \in D^{g,TR}$

call Image Retrieval ($D^g, I_l^{g,tr}, n_g, w_k, \phi_k^g$),

Loop

compute the fitness for ϕ_k^g which is the average of precision rates for each $I_l^{g,tr}$. save

parameters.

Loop

save best in ϕ_k^g

Loop

Step 5: Output Φ_0 ,

where $\{\phi_o^g | g = 1, 2, \dots, n_g\}$

$$\Phi_0 = \{((F_{C_{i_0}}^{g,tr}, d_{C_{i_0}}^{g,tr}), (F_{T_{j_0}}^{g,tr}, d_{C_{i_0}}^{g,tr}), (F_{C_{i_0}}^{g,tr}), F_{C_{i_0}}^{g,tr}) | g = 1, 2, \dots, n_g\}.$$

3.5 RESNET 50

Deep convolutional neural networks have achieved the human level image classification result. Deep networks extract low, middle and high-level features and classifiers in an end-to-end multi-layer fashion, and the number of stacked layers can enrich the “levels” of features. The stacked layer is of crucial importance, look at the ImageNet result. When the deeper network starts to converge, a degradation problem has been exposed: with the network depth increasing, accuracy gets saturated (which might be unsurprising) and then degrades rapidly. Such degradation is not caused by overfitting or by adding more layers to a deep network leads to higher training error. The deterioration of training accuracy shows that not all systems are easy to optimize. To overcome this problem, Microsoft introduced a deep residual learning framework. Instead of hoping every few stacked layers directly fit a desired underlying mapping, they explicitly let these layers fit a residual mapping. The formulation of $F(x)+x$ can be realized by feed forward neural networks with shortcut connections. The shortcut connections perform identity mapping, and their outputs are added to the outputs of the stacked layers. By using the residual network, there are many problems which can be solved such as:

- ResNets are easy to optimize, but the “plain” networks (that simply stack layers) shows higher training error when the depth increases.
- ResNets can easily gain accuracy from greatly increased depth, producing results which are better than previous networks.

Plain Network

The plain baselines (Fig. 2, middle) are mainly inspired by the philosophy of VGG nets (Fig. 2, left). The convolutional layers mostly have 3×3 filters and follow two simple rules:

1. For the same output feature map, the layers have the same number of filters;
2. If the size of the features map is halved, the number of filters is doubled to preserve the time complexity of each layer.
3. It is worth noticing that the ResNet model has fewer filters and lower complexity than VGG nets.

IV. PERFORMANCE MEASURES

An image region is said to be positive or negative, depending on the data type. Furthermore, a decision for the detected result can be either correct (true) or incorrect (false). Therefore, the decision will be one of four possible categories: true positive (TP), true negative (TN), false positive (FP), and false negative (FN). The correct decision is the diagonal of the confusion matrix.

4.1 Accuracy

Accuracy is the measure of a correct prediction made by the classifier. It gives the ability of performance of the whole classifier.

$$accuracy = \frac{TP + TN}{TN + FP + FN + TP}$$

4.2 Receiver Operating Characteristic (ROC)

The ROC analysis is a well-known evaluation method for detecting tasks. Firstly, a ROC analysis was used in medical decision-making; consequently, it was used in medical imaging. The ROC curve is a graph of operating points which can be considered as a plotting of the true positive rate (TPR) as a function of the false positive rate (FPR). The TPR and the FPR are also called sensitivity (recall) and specificity, respectively.

$$\text{sensitivity} = \frac{TP}{FN + TP}$$

$$\text{specificity} = \frac{TN}{TN + FP}$$

4.3 Area under the ROC Curve (AUC)

The AUC is used in the medical diagnosis system and it provides an approach for evaluating models based on the average of each point on the ROC curve. For a classifier performance the AUC score should be always between '0' and '1', the model with a higher AUC value gives a better classifier performance.

4.4 Precision

Precision is the ratio of correctly predicted positive observations to the total predicted positive observations. High precision relates to the low FPR. The precision is calculated using the following equation

$$\text{Precision} = \frac{TP}{TP + FP}$$

4.5 F1 Score

F1 score is the weighted average of precision and recall. It is used as a statistical measure to rate the performance of the classifier. Therefore, this score takes both false positives and false negatives into account.

$$F1\text{score} = \frac{2 * \text{Recall} * \text{Precision}}{\text{Recall} + \text{Precision}}$$

V. RESULT AND ANALYSIS

The performance parameters are calculated by comparing the segmented out with manually segmented images. Here, two segmentation techniques used for the detection of tumor from lung MRI have been studied extensively. In this thesis, we have examined the following segmentation techniques (i) Region Growing, (ii) Modified color based K-means clustering.

Segmentation outputs obtained for four different algorithm are given in figure 5.1. In this section the proposed method for benign and malignant tumor are shown in below figure.

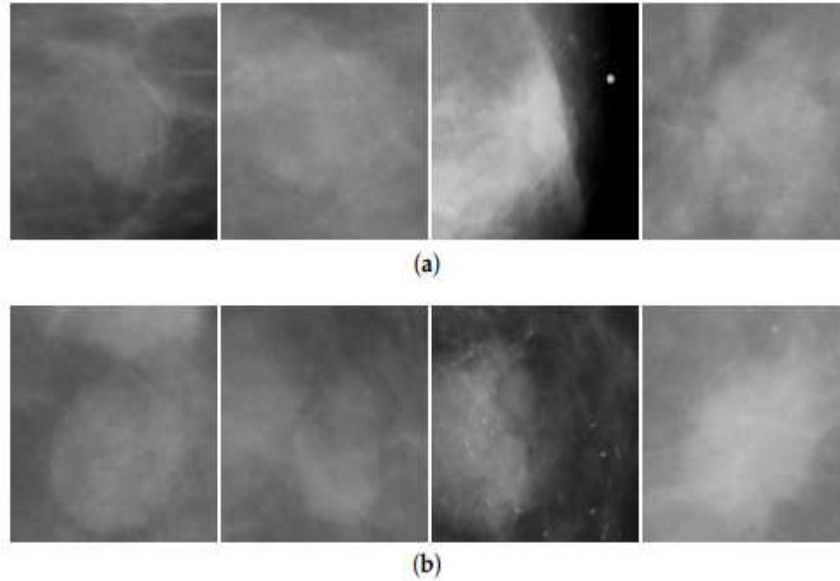


Figure 5.1: Experimental Result of Two Benign and Two Malignant Samples from (a) the Curated Breast Imaging Subset of DDSM (CBIS-DDSM) and (b) DDSM-400.

A system that detects Tumour by deep learning technique. This system provides an all-time solution to the diagnostics of tumour in breast cell. This proposed system has an average accuracy rate. The result of the proposed model is that we can use ResNet architecture to differentiate the affected tumour cells.

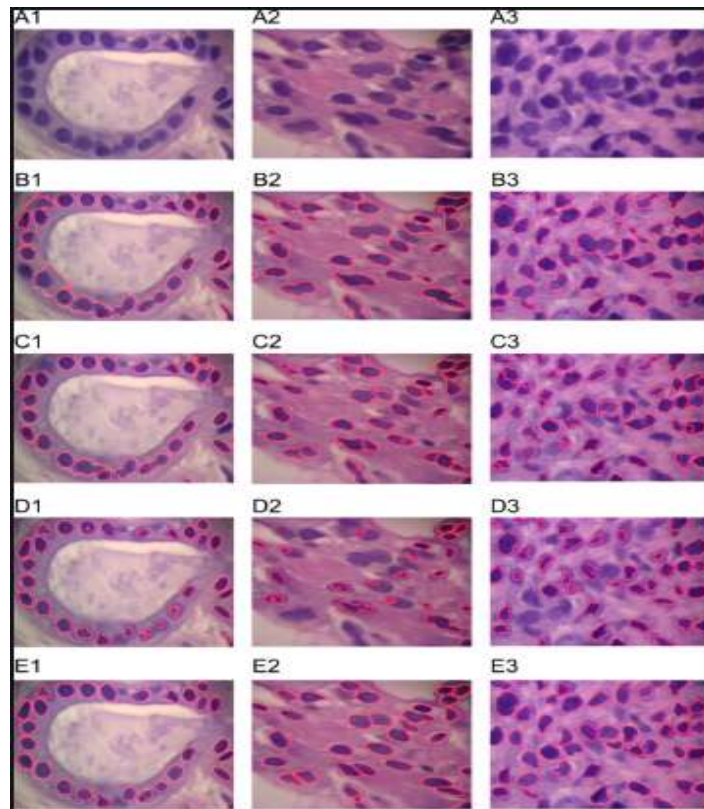


Figure 5.2: Segmented Images of Breast Tumor

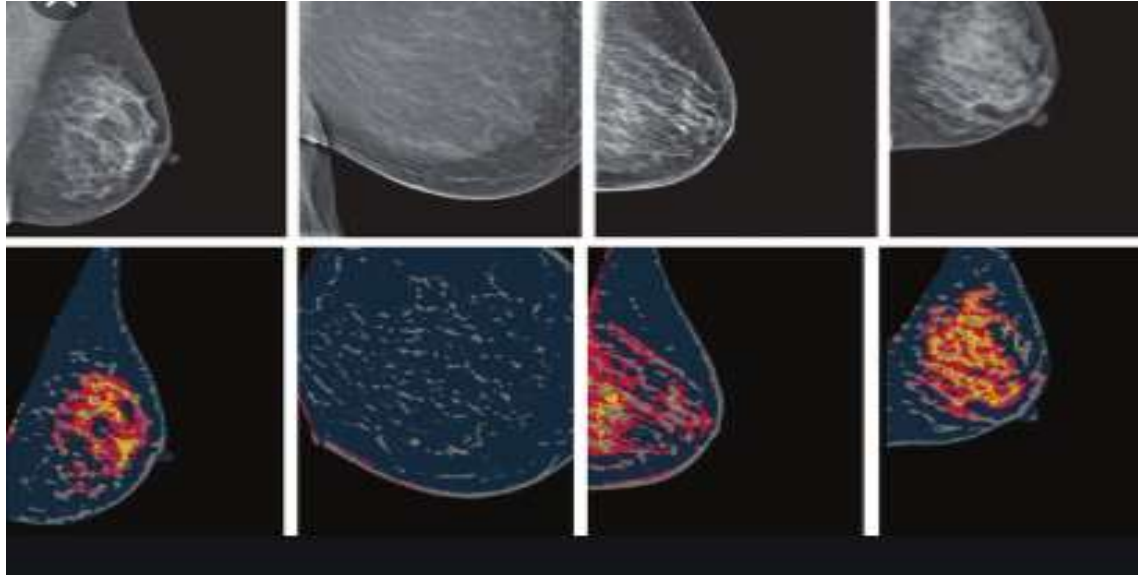


Figure 5.3(a): Experimental Result of Segmented Image for Benign Tumor

The Figure 5.3 (a) depicts the proposed method that obtains the input image by the sensors that indicates the input image. Next images indicate the pro-processed image (HE) and finally it depicts the region growing segmented image

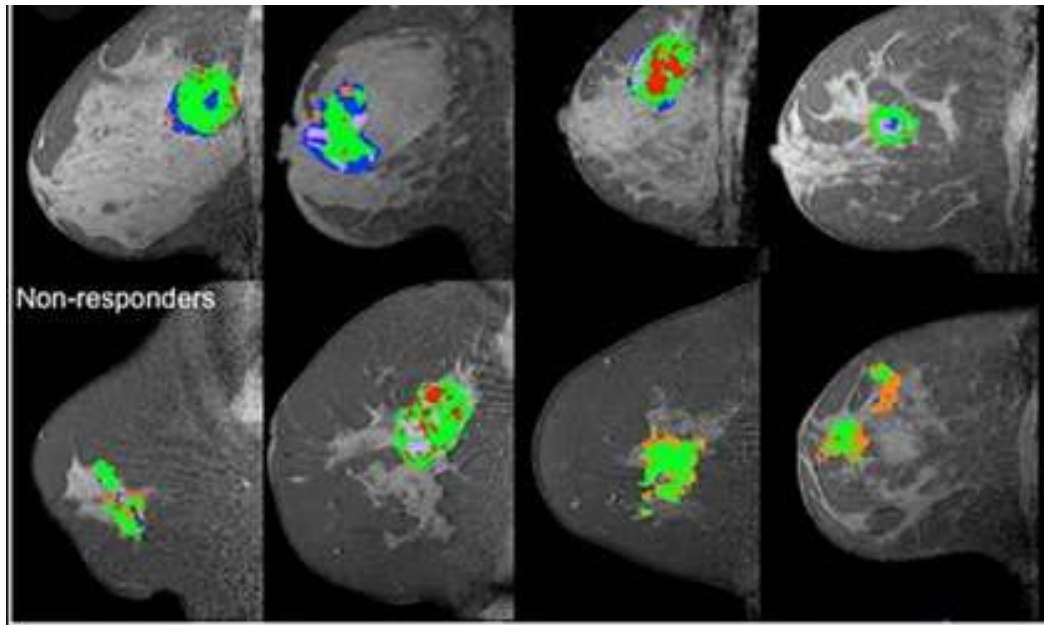


Figure 5.3(b): Experimental Result of Segmented Image for Malignant Tumor

The Figure 5.3 (b) depicts the proposed method that obtains the input image by the sensors that indicates the input image. Next images indicates the pro-processed image (HE) and finally it depicts the region growing segmented image

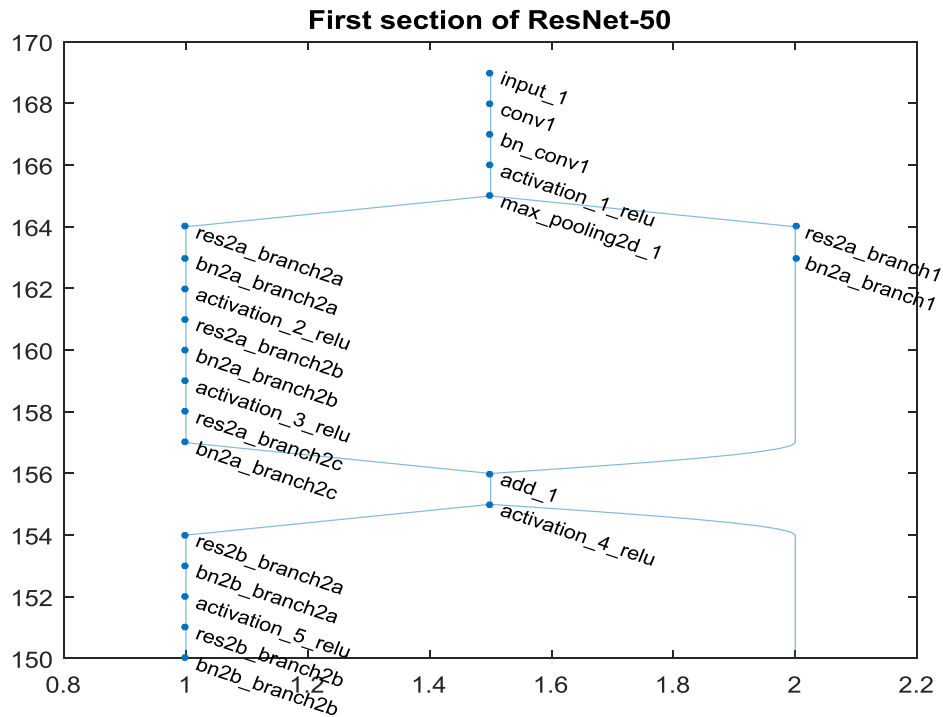
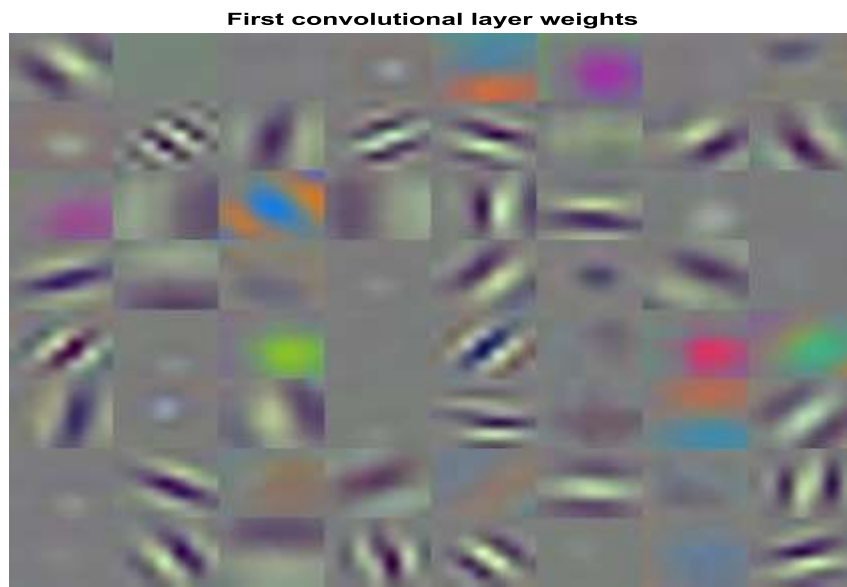


Figure 5.4: Resnet 50 Architecture



Confusion matrix is the graphical representation between the Target class and Output class. In this matrix the true positive values are denoted as green color box and the true negative value are shows in red box. Fig. 5.5 shows the output of CNN classifiers which are the customary metrics morals for numerous features. It is possible to recognize from table, which feature amalgamations provides higher accuracy. Border error symbolizes the rate of faultily breast images. This gives the lower accuracy of 90.00%.

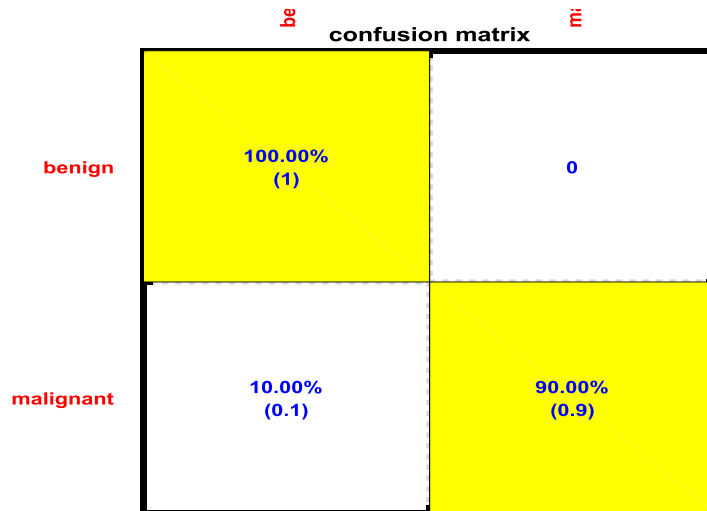


Figure 5.5 Confusion Matrix of CNN Classifier

Table 5.1: Analysis of Performances Parameters

Method	Accuracy (%)	Sensitivity (%)	Specificity (%)	PSNR	MSE
Region Growing	84.92	75.23	84.88	54.75	2.2114
Watershed	77.11	82.16	76.98	42.25	3.4968
Canny Edge detector	94.13	90.59	91.12	68.19	2.3998

As per the obtained outputs, it is clear that Canny edge detector segments tumor regions more similar to the existing images. Accuracy is an important parameters of a segmentation algorithm. Watershed algorithm has the lowest segmentation accuracy of 77.11% and highest segmentation accuracy of 94.13% is obtained for canny edge detector. The accuracy of the region growing is 84.92% Thus, from this comparison it is well cleared that proposed modified color based canny edge detector algorithm is the superior algorithm in terms of segmentation accuracy.

```

Command Window
New to MATLAB? See resources for Getting Started.

ans =
    0.9500

label =
    categorical
    benign

opt =
    struct with fields:
        mode: 'both'
        format: '8.2f'
        className: {'benign' 'malignant'}
        matPlotOpt: [1x1 struct]
    
```

For execution assessment, parameters of the proposed classification proposal such as characterization of specificity, sensitivity and accuracy of proposed method are calculated .The performance measures are as follows:-

1. Accuracy = $(TP+TN) / (TP+TN+FP+FN) * 100\%$
2. Specificity = $TN / (TN+FP) * 100\%$
3. Sensitivity = $TP / (TP+FN) * 100\%$ where
4. True positive (TP): Reported as lung tumor on MRI as well as biopsy.
5. True negative (TN): Not reported as lung tumor on MRI as well as biopsy.
6. False positive (FP): Reported as lung tumor on MRI but not on biopsy.
7. False negative (FN): Not reported as lung tumor on MRI but reported on biopsy.

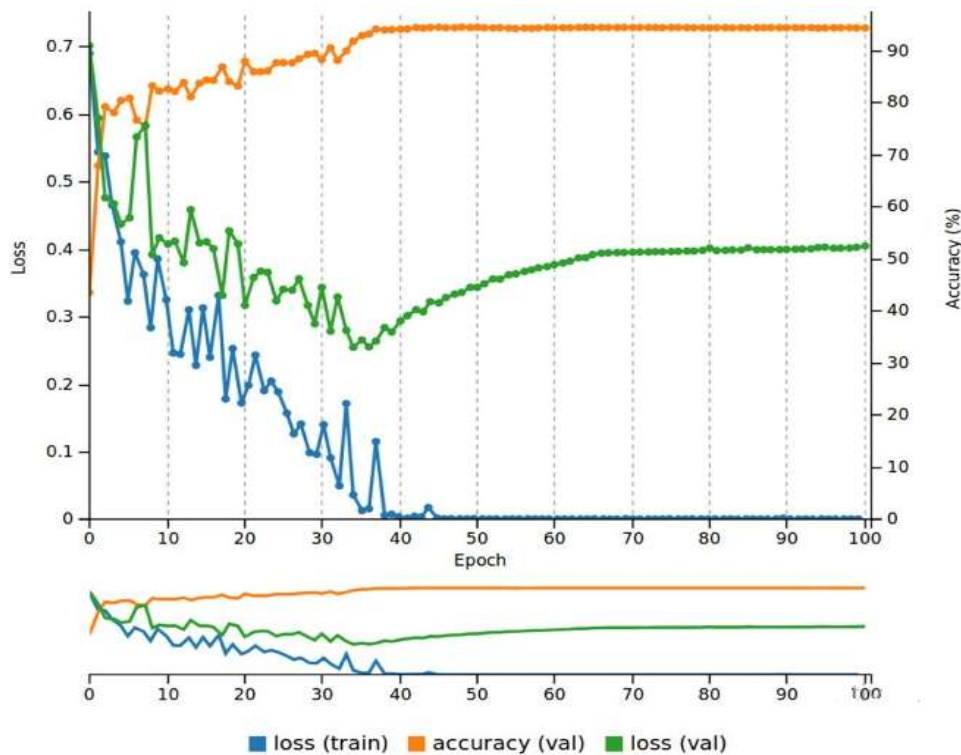


Figure 5.6: Performance Graph of Classifier

Table: 5.2: Shows the Performance Analysis of Proposed Method

Methods/ Benchmarks BPP	BPP	Existing Method			Proposed Method		
		PSNR	SSIM	CF	PSNR	SSIM	CF
(S.Singh& Siddiqui, 2013)	2	34.9	0.94	0.94	28	0.89	0.981
(V. Kumar & Kumar, 2017)	2	43	0.97	0.97	42	0.94	0.845
(Sathisha et al 2013)	4.6	41	0.956	0.962	26	0.954	0.946
(Kadhim., Premaratne, 2018)	5.4	48	0.924	0.910	32	0.845	0.987
(Kadhim, 2018)	3.2	46	0.922	0.936	33	0.9124	0.9950
Proposed Method	7.89	52.1	0.996	0.999	37.04	0.9254	0.997

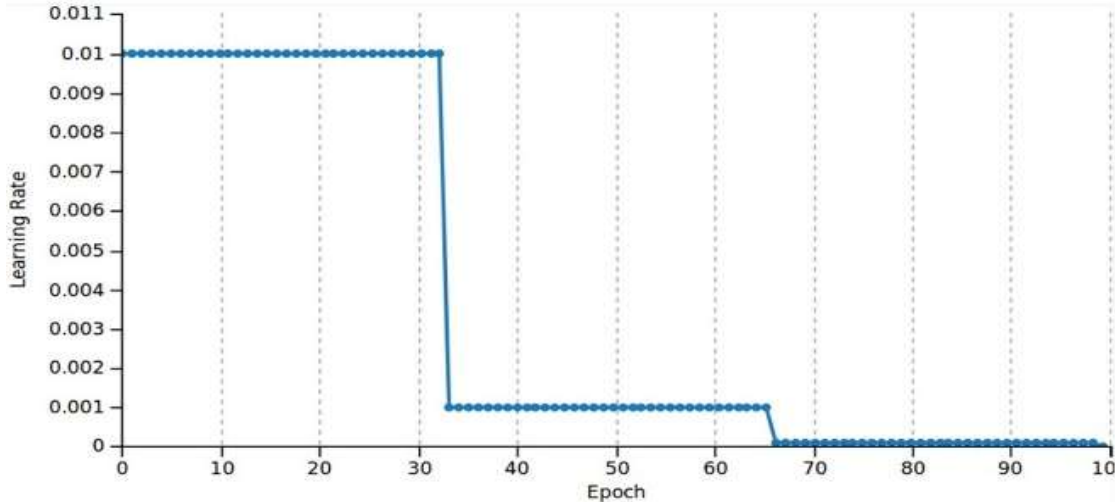


Figure 5.7: Resumes the Results throughout the Entire Training and Validation as well as the Learning Rate Behavior

After 100 epochs of training, we observed a descending behavior of the loss value until epoch 40. At epoch 100, the loss value for the validation was only 0.1 higher than the one at epoch 40; however, this steady increase of the loss function indicated that the AlexNet was starting to overfit at epoch 40. To overcome this issue, we used the weights saved in epoch 40 to test the performance of the network in the test dataset. Regarding, the validation dataset and before the CNN started to overfit, the network showed a performance of 94.35% of accuracy.

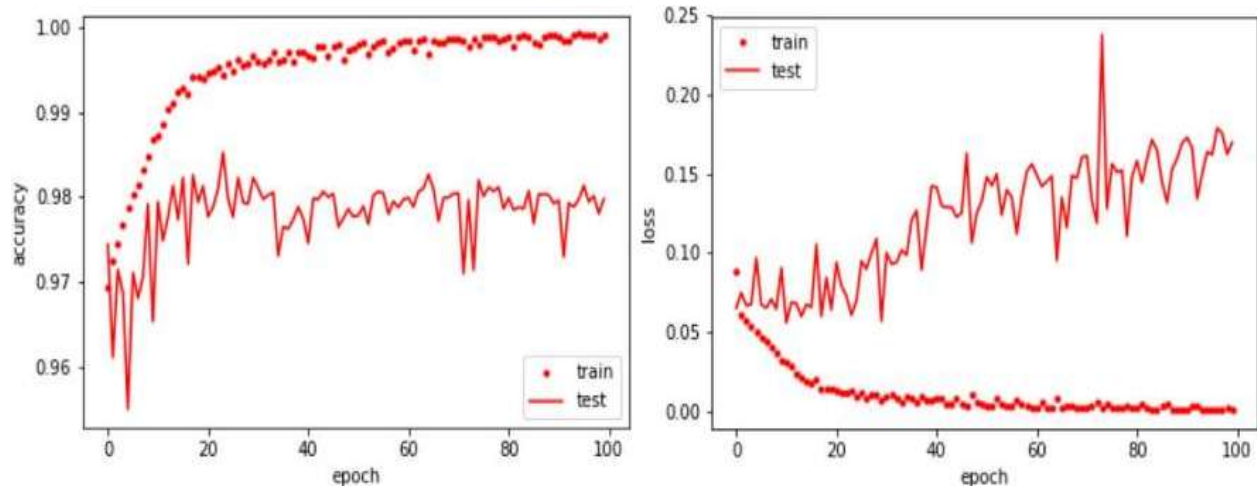


Figure 3 resume the performance of the network after 100 epochs of training. The overall accuracy was 97.98% in the validation patch dataset, and 97.73% in the testing patch dataset. Regarding the convergence using Adam optimizer, the loss value for both training and validation dataset showed a decreasing behavior. Similarly to the AlexNet, early stopping of the network was applied around epoch #24 due to the constant average loss value in the validation dataset and the increasing behavior afterward. In addition, the Dice coefficient, obtained in both validation and testing datasets, indicates that nearly 60% of the predicted mask overlaps with the ground truth.

VI. CONCLUSION

Early tumor detection, non-invasive tumor subtyping and treatment response evaluation present major challenges in the radiological work-up of patients at risk and patients who have already developed breast cancer. Intensified screening programs with state-of-the-art imaging techniques and advanced image post-processing algorithms are being developed and hold the potential to improve patient outcome. In this paper, the neural network is used in feature extraction and classification. By using the neural network, the accuracy performance provided better to comparing other machine learning techniques. The following explorations can be made by researches in future:

- In this CBIR system, only three features are considered as feature vector for image representation. Equal weightage is given to all the three features. In addition to this, more low level image descriptors (e.g. color, texture, shape etc.) may be considered as feature vector for image representation. Based on the property of features, due weightage may be given.
- Other optimization techniques such as Tabu search, Ants Colony algorithm etc., may be considered to measure the similarity between query and database images for indexing and retrieval. In addition to this, relevance feedback may be considered to increase the retrieval performance.

REFERENCES

- [1] A.B.Kanduri, A., P.V.Patil, P. and P.S.Mogale, P. (2016). Green Fodder Yield and Nutrient Composition of African Tall Maize Fodder (*Zea mays*) With Various Nitrogen-Phosphorus Levels. *International Journal of Advanced Engineering, Management and Science*, 2(5), pp.279-281.
- [2] Al-Ridha, N. and Jassim, Z. (2017). Seismic Study at Subba Oil Field Applying Seismic Velocity Analysis. *International Journal of Advanced Engineering Research and Science*, 4(11), pp.62-69.
- [3] Alto, Hilary, Rangaraj M. Rangayyan, Raman B. Paranjape, JE Leo Desautels, and Heather Bryant. "An indexed atlas of digital mammograms for computer-aided diagnosis of breast cancer." *In Annales des télécommunications*, vol. 58, no. 5-6, p. 820. Springer-Verlag, 2003.
- [4] Amerta, I. M. S., Sara, I. M., & Bagiada, K. (2018). Sustainable tourism development. *International Research Journal of Management, IT and Social Sciences*, 5(2), 248-254.
- [5] Anandakumar, H., & Nisha, K. (2015). Enhanced multicast cluster-based routing protocol for delay tolerant mobile networks. *International Journal of Information and Communication Technology*, 7(6), 676.
- [6] Arulmurugan, R., & Anandakumar, H. (2018). Region-based seed point cell segmentation and detection for biomedical image analysis. *International Journal of Biomedical Engineering and Technology*, 27(4), 273.
- [7] Bento, A. C. (2018). Internet of Things: An Experiment with Residential Automation for Robotics Classes. *International Research Journal of Management, IT and Social Sciences*, 5(2), 113-119. <https://doi.org/10.21744/irjmis.v5n2.51>
- [8] Bodake, S. (2016). Cloud Computing Load Balancing Algorithms Comparison Based Survey. *International Journal of Advanced Engineering, Management and Science*, 2(5), pp.282-287.
- [9] Cheng, Heng-Da, X. J. Shi, Rui Min, L. M. Hu, X. P. Cai, and H. N. Du. "Approaches for automated detection and classification of masses in mammograms." *Pattern recognition* 39, no. 4 (2006): 646-668.
- [10] Cheng, Heng-Da, Xiaopeng Cai, Xiaowei Chen, Liming Hu, and Xueling Lou. "Computer-aided detection and classification of microcalcifications in mammograms: a survey." *Pattern recognition* 36, no. 12 (2003): 2967-2991.
- [11] Dafik, D., Nurrohim, M., Fatahillah, A., P. M. and Susanto, S. (2017). The Air Flow Analysis of Coffee Plantation Based on Crops Planting Pattern of the Triangular Grid and Shackle of Wheel graphs by using a Finite Volume Method. *International Journal of Advanced Engineering Research and Science*, 4(11), pp.58-61.
- [12] Desfiandi, A., Suman Rajest, S., S. Venkateswaran, P., Palani Kumar, M., & Singh, S. (2019). Company Credibility: A Tool To Trigger Positive Csr Image In The Cause-Brand Alliance Context In Indonesia. *Humanities & Social Sciences Reviews*, 7(6), 320-331.

- [13] Dhivya V., Anandakumar H, & Sivakumar M. (2015). An effective group formation in the cloud based on Ring signature. 2015 *IEEE 9th International Conference on Intelligent Systems and Control (ISCO)*. doi:10.1109/isco.2015.7282366
- [14] Dr. P. Suresh and Suman Rajest S (2019), "An Analysis of Psychological Aspects in Student-Centered Learning Activities and Different Methods" in *Journal of International Pharmaceutical Research* , Volume: 46, Issue 01, Page No.: 165-172.
- [15] Dr. P.S. Venkateswaran, Dr. A. Sabarirajan, S. Suman Rajest And R. Regin (2019) "The Theory of the Postmodernism in Consumerism, Mass Culture and Globalization" in *The Journal of Research on the Lepidoptera* Volume 50 (4): 97-113
- [16] H, A., & K, U. (2018). Cooperative Spectrum Handovers in Cognitive Radio Networks. *EAI/Springer Innovations in Communication and Computing*, 47–63.
- [17] Haldorai, A., & Kandaswamy, U. (2019). Cooperative Spectrum Handovers in Cognitive Radio Networks. *EAI/Springer Innovations in Communication and Computing*, 1–18.
- [18] Haldorai, A., & Kandaswamy, U. (2019). Dynamic Spectrum Handovers in Cognitive Radio Networks. *EAI/Springer Innovations in Communication and Computing*, 111–133.
- [19] Haldorai, A., & Kandaswamy, U. (2019). Energy Efficient Network Selection for Cognitive Spectrum Handovers. *EAI/Springer Innovations in Communication and Computing*, 41–64.
- [20] Haldorai, A., & Kandaswamy, U. (2019). Intelligent Cognitive Radio Communications: A Detailed Approach. *EAI/Springer Innovations in Communication and Computing*, 19–40.
- [21] Haldorai, A., & Kandaswamy, U. (2019). Software Radio Architecture: A Mathematical Perspective. *EAI/Springer Innovations in Communication and Computing*, 65–86.
- [22] Jadhav, S. (2016). Load Balancing in Cloud Nodes. *International Journal of Advanced Engineering, Management and Science*, 2(5), pp.259-262.
- [23] K.B. Adanov, S. Suman Rajest, Mustagaliyeva Gulnara, Khairzhanova Akhmaral (2019), "A Short View on the Backdrop of American's Literature". *Journal of Advanced Research in Dynamical and Control Systems*, Vol. 11, No. 12, pp. 182-192.
- [24] Krizhevsky, Alex, Ilya Sutskever, and Geoffrey E. Hinton. "Imagenet classification with deep convolutional neural networks." In *Advances in neural information processing systems*, pp. 1097-1105. 2012.
- [25] Laghmati, Sara, Amal Tmiri, and Bouchaib Cherradi. "Machine Learning based System for Prediction of Breast Cancer Severity." In *2019 International Conference on Wireless Networks and Mobile Communications (WINCOM)*, pp. 1-5. IEEE.
- [26] Laksmiyanti, D. and Nilasari, P. (2017). Daylight Performance of Middle-rise Wide Span Building in Surabaya (Case Study: G-building ITATS). *International Journal of Advanced Engineering Research and Science*, 4(11), pp.77-83.
- [27] Lee, Rebecca Sawyer, Francisco Gimenez, Assaf Hoogi, Kanae Kawai Miyake, Mia Gorovoy, and Daniel L. Rubin. "A curated mammography data set for use in computer-aided detection and diagnosis research." *Scientific data* 4 (2017): 170177.
- [28] Lisa, O., & Hermanto, B. (2018). The effect of tax amnesty and taxpayer awareness to taxpayer compliance with financial condition as intervening variable. *International Research Journal of Management, IT and Social Sciences*, 5(2), 227-236.
- [29] Markosyan, L., Badalyan, H., Vardanyan, A. and Vardanyan, N. (2017). Peculiarities of a Colloidal Polysaccharide of Newly Isolated Iron Oxidizing Bacteria in Armenia. *International Journal of Advanced Engineering Research and Science*, 4(11), pp.70-76.
- [30] Martini, L. K. B., Suardana, I. B. R., & Astawa, I. N. D. (2018). Dimension Effect of Tangibles, Reliability, Responsiveness, Assurance, Empathy, Leadership towards Employee Satisfaction. *International Research Journal of Management, IT and Social Sciences*, 5(2), 210-215.
- [31] Md. Salamun Rashidin, Sara Javed, Bin Liu, Wang Jian, Suman Rajest S (2019), "Insights: Rivals Collaboration on Belt and Road Initiatives and Indian Recourses" in *Journal of Advanced Research in Dynamical and Control Systems*, Vol. 11, SI. 04, Page No.: 1509-1522.
- [32] Moschopoulos, Charalampos, Dusan Popovic, Alejandro Sifrim, Grigorios Beligiannis, Bart De Moor, and Yves Moreau. "A genetic algorithm for breast cancer diagnosis." In *International Conference on Engineering Applications of Neural Networks*, pp. 222-230. Springer, Berlin, Heidelberg, 2013.
- [33] Mythili, K., & Anandakumar, H. (2013). Trust management approach for secure and privacy data access in cloud computing. *2013 International Conference on Green Computing, Communication and Conservation of Energy (ICGCE)*. doi:10.1109/icgce.2013.6823567

- [34] P, S. and S, K. (2016). Information Upload and retrieval using SP Theory of Intelligence. *International Journal of Advanced Engineering, Management and Science*, 2(5), pp.274-278.
- [35] Pace, Lydia E., and Nancy L. Keating. "A systematic assessment of benefits and risks to guide breast cancer screening decisions." *Jama* 311, no. 13 (2014): 1327-1335.
- [36] Petersen, Kersten, Konstantin Chernoff, Mads Nielsen, and Andrew Y. Ng. "Breast density scoring with multiscale denoising autoencoders." *In Proceedings of the MICCAI Workshop on Sparsity Techniques in Medical Imaging*. 2012.
- [37] R S, D. and M N, P. (2016). Software CrashLocator: Locating the Faulty Functions by Analyzing the Crash Stack Information in Crash Reports. *International Journal of Advanced Engineering, Management and Science*, 2(5), pp.269-273.
- [38] Rajest, S. S., Suresh, D. (2018). The Deducible Teachings of Historiographic Metafiction of Modern Theories of Both Fiction and History. *Eurasian Journal of Analytical Chemistry*, 13(4), emEJAC191005.
- [39] Rusandy, D. S., Astuti, W., & Firdiansjah, A. (2018). Effect of MCSQ and COSE on service recovery and its impact on customer satisfaction. *International Research Journal of Management, IT and Social Sciences*, 5(2), 237-247.
- [40] Russo, Fabrizio. "Recent advances in fuzzy techniques for image enhancement." *IEEE Transactions on Instrumentation and measurement* 47, no. 6 (1998): 1428-1434.
- [41] Sari, D. M. F. P., & Pradhana, I. P. D. (2018). Brand name, image, word of mouth towards buying habits and customer loyalty online shop. *International Research Journal of Management, IT and Social Sciences*, 5(2), 216-226.
- [42] Sharma, P., Rajendra .S, D. and C.N, V. (2016). A Comparative Study on Effects of Regular and Irregular Structures Subjected to Lateral Loading by Equivalent Static Method and Response Spectrum Method. *International Journal of Advanced Engineering, Management and Science*, 2(5), pp.263-268.
- [43] Soumokil, H. and Nara, O. (2017). Study of Irrigation Water Supply Efficiency to Support the Productivity of Farmers (Case Study at Kobisonta North Seram Central Maluku District). *International Journal of Advanced Engineering Research and Science*, 4(11), pp.49-57.
- [44] Suman Rajest S, Dr. P. Suresh (2018), "Absurd Realism And Structure In Thomas Pynchon's The Crying Of Lot 49" in *Journal of Advanced Research in Dynamical and Control Systems*, Vol.10, SI.11, Page No.: 571-580.
- [45] Suman Rajest S, Dr. P. Suresh (2018), "The Problematizing of History Concentrated on The Poetics of Historiographic Metafiction by Postmodernism and How It Influences Postmodern Fiction" in *International Journal of Pure and Applied Mathematics*, Vol.119, SI.16, Page No.: 2457-2469.
- [46] Suman Rajest S, Dr. P. Suresh (2018), "Themes and Techniques from Modernism to Postmodernism: The Dubious Continuance of Gravity's Rainbow" in *International Journal of Pure and Applied Mathematics*, Vol.119, SI.16, Page No.: 2373-2384.
- [47] Suman Rajest S, Dr. P. Suresh (2019), "The Dialog On Postmodernism Intertextuality, Parody, The Talk Of History And The Issue Of Reference" in *International Journal of Recent Technology and Engineering*, Vol.7, Issue-5C, Page No.: 244-251.
- [48] Suman Rajest S, Dr. P. Suresh, "An Analysis of Chetan Bhagat's Revolution -2020: Love, Ambition, Corruption" in *International Journal of English Language, Literature in Humanities (IJELLH)*, Volume: V, Issue IX, September 2017, Page No.: 52-62.
- [49] Suman Rajest S, Dr. P. Suresh, "Galapagos: Is Human Accomplishment Worthwhile" in *Online International Interdisciplinary Research Journal*, Volume: VII, Special Issue II, September 2017, Page No.: 307-314.
- [50] Suman Rajest S, Dr. P. Suresh, "The white Tiger by Aravind Adiga: Depiction of Fermentation in Society" in *International Journal of Information Movement*, Volume: II, Special Issue VI, October 2017, Page No.: 189-194.
- [51] Venkatesh, C., Chaitanya, B. and Yadav, K. (2017). Some aspects of Cold Deformation studies of Al-ZrB₂ composites. *International Journal of Advanced Engineering Research and Science*, 4(11), pp.40-48.
- [52] Wang, Jinhua, Xi Yang, Hongmin Cai, Wanchang Tan, Cangzheng Jin, and Li Li. "Discrimination of breast cancer with microcalcifications on mammography by deep learning." *Scientific reports* 6, no. 1 (2016): 1-9.
- [53] Yang, Zhicheng, Zhenjie Cao, Yanbo Zhang, Rwei-Sung Lin, Shibin Wu, Lingyun Huang, Mei Han, and Jie Ma. "Deep Learning Based Mass Detection in Mammograms." (2019).